

Kinematics of deformation in the Tibetan Plateau and its margins constrained by GPS measurements

Pei-Zhen Zhang and Zhijun Niu

State Key Laboratory of Earthquake Dynamics, Institute of Geology,
China Earthquake Administration, Beijing 100029, China

Abstract

As the most prominent example of large-scale continental deformation, Tibetan Plateau offers an ideal natural laboratory for quantifying such deformation and understanding the relevant dynamic processes. GPS provides a powerful means to directly measure the kinematics of present-day deformation. Our synthesis of GPS velocities from 553 stations in Tibetan Plateau and its margins quantitatively show that most of the relative India/Eurasia motion has been accommodated primarily by crustal shortening along the margins, strike-slip and normal faulting in the plateau interior, and clockwise rotation around the eastern end of Himalaya. The eastward extrusion of Tibetan Plateau out of India's northward pass is carried out by roughly eastward flow of crustal material rather than by rigid block rotation. To the east, the eastward flow of crustal material causes shortening across the eastern margin of the plateau and clockwise rotations where resistance to such flow may be weak. The present-day tectonics in the Tibetan Plateau is best described as deformation of a continuous medium, at least when averaged over distances of ~100 km.

Introduction

The Tibetan Plateau, the world's largest and highest plateau, has been growing and evolving since the collision and subsequent penetration of the India with Eurasia 50 million years ago (Molnar and Tapponnier, 1975; Rowley, 1996). How the Tibetan Plateau deforms in response to the collision, however, remains enigmatic and subject to debate, with rigid plates or blocks, continuous deformation of the entire lithosphere, and flow in the lower crust providing keys to its understanding (Tapponnier et al., 1982, 2001; England and Houseman, 1986; Molnar et al., 1993; England and Molnar, 1997; Royden et al., 1997; Holt et al., 2000; Flesch et al., 2001). Unfortunately, much of the region is remote, and a complete kinematic description of deformation over the entire Tibetan Plateau has not been available until recently. Dynamic models intended to explain deformation of the Tibetan Plateau need to be tested in terms of kinematics. Global Positioning System (GPS), developed in last decade with the successful operation of International GPS Service (IGS), provides a powerful means to directly measure the kinematic pattern of present-day crustal deformation in remote and large-scaled region like the Tibet (Chen et al., 2001; Wang et al., 2001; Chen et al., 2003; Calais et al., 2003; Zhang et al., 2004). We, in this paper, synthesis GPS studies in the Tibetan Plateau and its margins (Paul et al., 2001; Wang et al., 2001; Banerjee and Burgmann, 2002) to show in which ways the collision between India and Eurasia is accommodated and to shed new insights into the dynamics of its contemporary tectonic deformation. We designate this paper to the decadal anniversary of IGS for its excellent service to the researches of geodynamics.

Data and data process

Significant advancement for the monitoring of crustal deformation in the Tibet Plateau was accomplished in 1998 when the Crustal Motion Observation Network of China (CMONOC) was established. The principal data used for this study come from the CMONOC collected during 1998 and 2002, including 25 continuous stations, 56 annually observed stations with an occupation of at least 7 days (~168 hours' data collection) in each survey, and 961 regional stations observed in 1999 and 2001 with an occupation of at least 3 days (~72 hours' data collection) in each survey.

The data were processed in four steps (Shen et al., 2000, 2001). First, we put the observation data together to solve for the daily loosely-constrained station coordinates and satellite orbits using the

GAMIT software (King and Bock, 1995). Second, we combined the regional daily solution with the loosely constrained global solutions of ~80 IGS tracking stations produced at the Scripps Orbital and Position Analysis Center (Bock et al., 1997) using the GLOBK software (Herring, 1995). The merged daily solution includes the loosely constrained station coordinates, polar motion and satellite orbit parameters, and the variance-covariances matrix. Third, we estimated station positions and velocities in the ITRF2000 reference frame using the QOCA software (Dong et al., 1998). The QOCA modeling of the data was done through sequential Kalman filtering, allowing adjustment for global translation and rotation of each daily solution. In the last step, we transformed the velocity solution to a Eurasia-fixed reference frame using the angular velocity of Eurasia with respect to the ITRF deduced from 11 IGS stations (NYAL, ONSA, HERS, WSRT, KOSG, WTZR, VILL, GLSV, IRKT, TIXI) in the stable Eurasia plate [Shen et al., 2000; 2001].

Besides the CMONOC data, we collected three additional data sets of station velocities from Paul et al. [2001], Wang et al. [2001], and Banerjee and Burgmann (2002) to increase the coverage and station density of the India, Himalayan and central Tibetan regions. Paul et al. (2001)'s velocity data (13 stations in India and the Himalaya) are in an India-fixed reference frame, whereas Wang et al. (2001)'s velocity data (41 stations distributed in India, the Himalaya, and central Tibet) and Banerjee and Burgmann' (2002)'s (24 stations in the western Himalaya) are in a Eurasia-fixed reference frame, which differs slightly from the above Eurasia-fixed reference frame we employed. As each of the additional velocity data sets has some common stations with the CMONOC data set, we chose common stations for the three data sets, to transform them to the Eurasia-fixed reference frame of the CMONOC data set, by minimizing the velocity differences of the common stations in the corresponding reference frames. After the transformation, the maximum difference of the velocities for each common station in different data sets is less than 2.9 mm/yr and 2.6 mm/yr for the east and north components, respectively, which are within the 2 standard deviations of the velocity components. Thus, we calculated the weighted average of the velocity components for the common stations and estimated their standard deviations. We finally obtain velocities for 553 stations in the Tibetan Plateau and its margins, that provide adequate coverage to interpret the magnitude and style of deformation despite of void areas in northwestern corner of the plateau (Fig. 1).

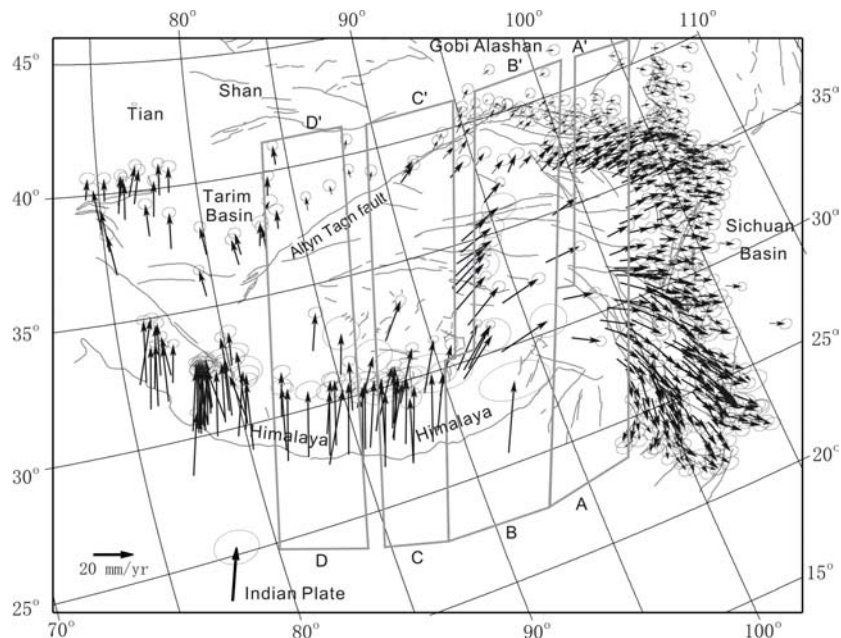


Figure 1. GPS velocity vectors (mm/yr) in the Tibetan Plateau and its margin with respect to the stable Eurasia, The ellipses denote the region of 1-sigma error. The polygons show locations of the profiles, and GPS stations covered by each profile.

Shortenings across the Tibetan Plateau and its margins

The Tibetan Plateau and its margins, including the Himalaya, the Altyn Tagh and the Qilian Shan, undergo substantial shortening. We draw four profiles (A-A', B-B', C-C' and D-D') across the plateau along the N20°E direction, the inferred India-Eurasia convergence direction (Sella et al., 2002), to calculate the shortening across different parts of the plateau. The total shortenings between India and Tarim in this direction are 28 ± 2.5 , 33 ± 2.0 , and 34 ± 3.0 mm/yr along profiles D-D', C-C' and B-B' respectively (Fig. 2). The shortening seems to be slightly larger than 34 ± 4.0 mm/yr, if the Shilong Hill is regarded as part of the Himalaya, between the India and Gobi Alashan along profile A-A' (Figs. 1&2). Taking 36-40 mm/yr as total relative motion between India and Eurasia, the eastern Tibetan Plateau and its margins (Profiles A-A' and B-B') accommodates 85-94% of the total motion, whereas western Tibet (Profiles C-C' and D-D') absorbs 70-91% of total convergence and the rests are taken up by shortening across the Tianshan in the north (Abdrakhmatov et al. 1996; Reigber et al., 2001).

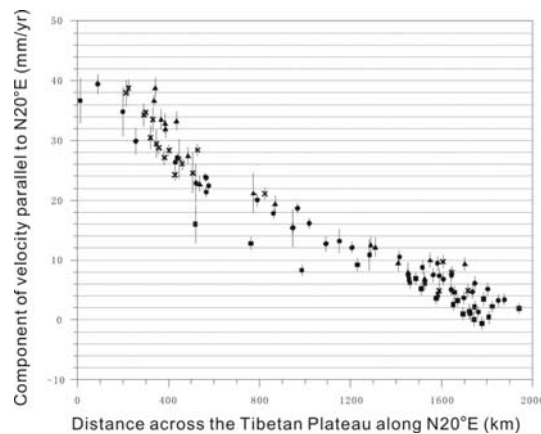


Figure 2. Velocity components parallel to N20°E vs. distance in km along each of 4 profiles in Fig. 1. Squares, diamonds, crosses and triangles show profile A-A', B-B', C-C' and D-D' respectively.

Partitions of the shortenings in the Himalaya, the northern margin, and the plateau interior

The N20°E convergence across the western Himalaya is 16 ± 2.5 mm/yr along profile D-D' (80°-84°E), slightly less but approximating previous geological (Lavé and Avouac, 2001) and geodetic (Bilham et al., 1996; Larson et al., 1999; Paul et al., 2001; Banerjee and Bürgmann, 2002) findings. To the east, the shortening rates across the Himalaya are 15 ± 3.0 and 14 ± 3.0 mm/yr along profiles C-C' and B-B' respectively (Fig. 2). The shortening along profile A-A' is not well constrained because of the poor station coverage and the influence by rotation of crustal material around the eastern Himalaya syntaxis (Fig. 1). We estimate 15-20 mm/yr shortening rate across the Himalaya along profile A-A'.

The northern margin of Tibet absorbs only slow convergence: 5.3 ± 1.0 and 6.2 ± 1.5 mm/yr parallel to N20°E on profiles C-C' and B-B' (Figs. 2 and 3), which includes left-lateral strike slip at 5.6 ± 1.6 and 5.0 ± 2.0 mm/yr parallel to the Altyn Tagh fault and 2.9 ± 1.8 and 3.2 ± 1.5 mm/yr of convergence perpendicular to the margin of Tibet (Fig. 3). These strike-slip and convergence rates along the eastern third of the northern plateau margin (profiles B-B' and C-C') are consistent with geological (Working Group on the Altyn Tagh fault, 1993) and other geodetic (Bendick et al., 2000; Wang et al., 2001; Shen et al., 2001) results. Shortening occurs at 6.0 ± 1.5 and 5.5 ± 1.8 mm/yr across the northeastern edge of the Tibetan Plateau perpendicular to the western and eastern Qilian Shan respectively (Fig. 3).

The amounts of shortening must be accommodated by the plateau interior are 11.3 ± 5.0 , 14 ± 3.0 , 12.7 ± 3.0 , and 10 ± 3.0 mm/yr along profile A-A', B-B', C-C', and D-D' respectively (Figs. 2 and 3). These velocity profiles show general feature of linear gradients except profile A-A' that may be significantly affected by rotations around the eastern Himalaya syntaxis (Figs. 1 & 3). However, views on how the shortening in the plateau interior is accommodated are still diverse, with the rigid block extrusion (Armijo

strain rate using the velocities of 17 stations located within the plateau interior indicate that the average N20°E contraction strain rates range from $(-1.3 \pm 0.4) \times 10^{-8}$ to $(-1.8 \pm 0.4) \times 10^{-8} \text{ yr}^{-1}$, and the average orthogonal extensional strain rate is $(2.1 \pm 0.3) \times 10^{-8} \text{ yr}^{-1}$.

The straining associated with the eastward transfer of crustal material can be illustrated by lateral movements orthogonal to the inferred India/Eurasia motion (Fig. 4). Lateral motions along profile A-A' and B-B' in the eastern Tibet increase steadily northward from the Himalayan across the breadth of southern Tibet and then decrease further north across the broad northeastern Tibetan Plateau into the stable Gobi Alashan region (Fig. 4). The fastest east-southeastward motion occurs at latitudes of 31°N -33°N and 33°N-35°N along profiles A-A' and B-B' respectively. The core of rapid eastward flow of crustal material in the central plateau is bounded by two shear zones, several hundred kilometers wide: right-lateral in the southern Tibetan plateau and left-lateral in central and northern Tibetan Plateau (Fig. 4). In profile A-A', the right-lateral shear clearly exists, but is difficult to calculate due to lack of stations. The left-lateral shear is $7.3 \pm 1.5 \text{ mm/yr}$ in the northern plateau interior. In profile B-B', the right-lateral shear is $13 \pm 2.0 \text{ mm/yr}$ and the left-lateral shear is $10 \pm 1.5 \text{ mm/yr}$. These right-lateral and left-lateral shears are accommodated by distributed faults with right-lateral strike-slip in the southern plateau (Armijo et al., 1989; Institute of Geology, 1993) and with left-lateral slip in the northern plateau respectively (Kidd and Molnar, 1988; Institute of Geology, 1993).

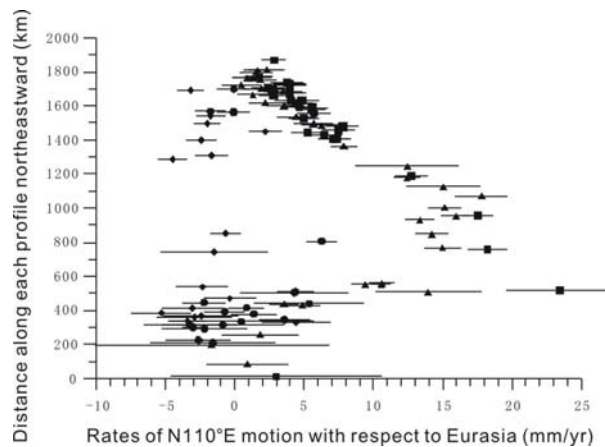


Figure 4. Velocity components normal to N20°E, the inferred India/Eurasia relative motion. Squares, triangles, dots and diamonds show profile A-A', B-B', C-C' and D-D' respectively.

The flow of Tibetan crustal material rotates around the eastern Himalaya syntaxis, causing southeastward to southward and even southwestward velocities observed in southern and western Yunnan province of China (Fig. 1). In addition to the rotation around the Eastern Himalayan Syntaxis reported previously (Le Dain et al., 1984; Molnar and Lyon-Caen, 1989; Holt et al., 1995; King et al., 1997; Royden et al., 1997; Wang et al., 2001), our data show that clockwise rotation involves the entire eastern part of the Tibetan Plateau. This kind rotation fundamentally differs from the rigid block rotation successfully describing plate motion, because for rigid-body movement, rates increase away from the rotation axis, and this seems opposite from velocity field in Fig. 1. Instead it probably relates to the eastward flow of crustal material away from internal parts of the plateau in response to the northward movement of India and southern Tibet with respect to southeastern China (Le Dain et al., 1984; Molnar and Lyon-Caen, 1989; King et al., 1997; Royden et al., 1997; Wang et al., 2001).

Eastward shortening in the eastern margin

Eastward transfer of crustal material from the plateau interior also implies roughly eastward shortening along its eastern margin (Fig. 3). The northern segment of the eastern margin is the

N15°W-trending Liupan Shan that also forms the eastern end of the northeastern margin of the plateau, where folding and thrust faulting take place (Zhang et al., 1991). A velocity profile perpendicular to the Liupan Shan indicates 7 ± 2 mm/yr shortening in the direction of N75°E (Zhang et al., 2004). The central segment, the Longmen Shan with a sharp geomorphic expression of the plateau margin, trends N32°E. King et al. (1997) and Chen et al. (2001) show absence of convergence across it. Wang et al. (2001) find 5 to 11 mm/yr velocity difference across the Longmen Shan, but interpret it has being accommodated by clockwise rotation around the eastern Himalaya syntaxis. Our velocity profile orthogonal to the Longmen Shan gives a 4 ± 2 mm/yr velocity difference in N122°E direction which we think has been absorbed by shortening along the margin itself (Zhang et al., 2004). The southern segment of eastern margin of the plateau is the Sichuan-Yunnan region where the Tibetan Plateau gradually grades into South China without obvious topographic boundary (Zhang et al., 2004). We draw an east-west profile across this segment. The velocity profile shows 7.5 ± 3.0 mm/yr east-west shortening (Zhang et al., 2004). It seems that the shortening across the eastern margin of Tibetan Plateau and clockwise rotation together absorb the eastward flow of crustal material from the plateau interior.

Westward motion in the western margin

The N20°E shortening ranges from 19 to 23 mm/yr or 21 ± 4.0 mm/yr across the western margin of the Tibetan Plateau (Fig. 1). Most of the shortening, however is taken up by the western Himalaya, whereas the interior of Tibetan Plateau only absorbs 4 ± 1 mm/yr. The lateral motions orthogonal to the inferred India/Eurasia motion also show steady increases northward across the Himalaya to the Tarim, but the direction of motion is westward as noted by Banerjee and Burgmann (2002) rather than eastward in the eastern Tibetan Plateau.

The Karakorum fault contributes to westward motion of the western margin of Tibetan Plateau. But the right-lateral slip rate on the fault is not well constrained with 32 ± 8 mm/yr (Avouac and Tapponnier, 1993), 11 ± 4 mm/yr (Banerjee and Burgmann, 2001), ~ 10 mm/yr (England and Molnar, 1997; Holt et al., 2000), ~ 6 mm/yr (Murphy et al., 2000), and 4 ± 1 mm/y (Brown et al., 2002). Our GPS measurements indicate that the velocity difference parallel to the fault is only ~ 4 mm/yr across the northern segment. This rate agrees well with geological study by Brown et al. (2002). Further to the south, we estimate 4 to 8 mm/yr or 6 ± 2 mm/yr right-lateral slip rate across the southern segment of karakorum fault. Together with recent determined lower slip rate along the Altyn Tagh (Bendick et al., 2000; Shen et al., 2001; Wang et al., 2001) and lower speed of westward motion of the western Tibetan Plateau, we think our rates on the Karakorum fault fit well in the kinematic system of present day deformation in the Tibetan Plateau and its margins.

Rigid-block like versus viscous-fluid like deformation

How the Tibetan Plateau deforms in response to the collision is subject to debate, with two end-member views of rigid plate-like (Tapponnier et al., 2001) and viscous fluid-like (Houseman and England, 1993) deformation of the lithosphere offering keys to its understanding. The GPS constraints on the kinematics of the Tibetan Plateau described above offer tests of plate-like and fluid-like descriptions of the kinematics (Fig. 4). As predicted by the fluid-like model (e.g. England and Houseman, 1986; Houseman and England, 1993; Holt et al., 2000), the N20°E convergence across the Tibetan Plateau and its edges absorbs a large fraction (70-94%) of India's northward penetration.

Surface velocities across boundaries between rigid blocks should vary discontinuously compared with smooth variations in both rates and directions, if large rigid bodies are absent. If dimensions of blocks are as large as 300-500 km (or more), as some argue for Asia and given fault locking depths of 10-20 km, GPS measurements at control points spaced at distances of tens of kilometers can test whether such blocks exist or not. The 10-12 mm/yr of left-lateral shear are distributed over a ~ 400 -km-wide zone spanning the Kunlun fault, a rate consistent with geologically inferred slip rates on that fault (Kidd and Molnar, 1988). Either interseismic locking to a large depth of > 25 km or a very low-viscosity lower crust (Zhang et al., 2004) would be required to assign all of this broadly distributed deformation to elastic strain

associated with slip on the Kunlun fault alone. Moreover, other active faults have been mapped within the 400-km-wide deformation zone that might accommodate some of the measured deformation. In any case, because of the ESE-WNW extension in the region between the shear zones, they cannot bound two rigid blocks, but rather seem to mark zones of more concentrated shear than elsewhere along profiles A-A' and B-B'. Crustal shortening across the Qilain Shan distributes in a zone of about 300~350 km width (Zhang et al., 2004). Across Liupan Shan, the northeastern margin, velocities gradually decrease across about 300 km wide zone (Zhang et al., 2004). In the eastern margin across the Longmen Shan, the about 4 mm/yr shortening forms approximate 200 km belt (Zhang et al., 2004). All of these cannot be matched by slips along a particular fault giving a reasonable locking depth and viscosity at depth, and therefore reject the model of rigid block extrusion.

Conclusion

The kinematics of contemporary deformation of the Tibetan Plateau in response to India/Eurasia collision involves crustal shortening along the margins, normal and strike-slip faulting in the interior and clockwise rotation of crustal material in the eastern part of Himalaya. To the west, the westward motion of the western margin of the plateau is observed with only 4 mm/yr slip rate. To the east, the eastward flow of crustal material causes shortening across the eastern margin of the plateau and clockwise rotations where resistance to such flow may be weak. The present-day tectonics in the Tibetan Plateau is best described as deformation of a continuous medium, at least when averaged over distances of ~100 km.

Acknowledgements:

This work has been supported by National Science Foundation of China, National Key Basic Research Program, and National Major Scientific Infrastructure Program. We thank Ruth Neilan for encouragements.

References

- Abdrakhmatov, K. Y. et al. Relatively recent construction of the Tien Shan inferred from GPS measurements of present-day crustal deformation rates. *Nature* 384, 450-453 (1996).
- Armijo, R., P. Tapponnier, and Han Tonglin, Late Cenozoic right-lateral strike-slip faulting in southern Tibet, *J. Geophys. Res.*, 94, 2787-2838, 1989.
- Avouac, J. P., and P. Tapponnier, Kinematic model of active deformation in central Asia, *Geophys. Res. Letters*, 1993, 20: 895-898.
- Banerjee, P. & Burgmann, R. Convergence across the northwest Himalaya from GPS measurement. *Geophys. Res. Lett.* 29, 2002.
- Bendick, R., et al., Geodetic evidence for a low slip rate in the Altyn Tagh fault system, *Nature*, 404, 69-72, (2000).
- Bilham, R. et al. GPS measurements of present-day convergence across the Nepal Himalaya. *Nature* 386, 61~64 (1997).
- Bock, Y. et al. Southern California Permanent GPS Geodetic Array: Continuous measurements of regional crustal deformation between the 1992 Landers and 1994 Northridge earthquakes. *J. Geophys. Res.* 102, 18013-18033 (1997).
- Brown, E. T., et al., Slip rates of the Karakorum fault, Ladakh, India, determined using cosmic ray exposure dating of debris flows and moraines, *J. Geophys. Res.*, 107, 2192, doi:10.1029/2000JB000100, (2002).
- Burchfiel, B. C., et al. Tectonics of the Longmen Shan and adjacent regions, Central China, *International Geology Review* 37, 661-735 (1996).
- Chen, Z. et al. Global Positioning System measurements from eastern Tibet and their implications for India/Eurasia intercontinental deformation. *J. Geophys. Res.*, 109, B01403, doi:10.1029/2002JB002151, 2004.
- Chen, Q., et al., A deforming block model for the present-day tectonics of Tibet, *J. Geophys. Res.* 108, NO. B10, 2501, doi:10.1029/2002JB002373, (2003).
- Calais, E. et al. GPS measurements of crustal deformation in the Baikal-Mongolia area (1994-2002): Implications for current kinematics of Asia, *J. Geophys. Res.* 108, NO. B10, 2501, doi:10.1029/2002JB002373, (2003).
- Clark, M.K. & Royden, L. H. Topographic ooze: Building the eastern margin of Tibet by lower crustal flow. *Geology*,

- 28, 703-706 (2000).
- Dong, D., Herring, T. A., & King, R. W. Estimating regional deformation from a combination of space and terrestrial geodetic data. *J. Geod.* 72, 200–214 (1998).
- England, P., and P. Molnar, Active deformation of Asia: from kinematics to dynamics, *Science*, 278, 647-650, 1997
- Flesch, L. M., A. J. Haines, and W. E. Holt, Dynamics of the India-Eurasia collision zone, *J. Geophys. Res.*, 106, 16,435-16,460, 2001.
- Herring, T. A. GLOBK: Global Kalman filter VLBI and GPS analysis program, version 4.0, Mass. Inst. of Technol., Cambridge, 1995.
- Holt, W. E. et al. Velocity field in Asia inferred from Quaternary fault slip rates and Global Positioning System observations. *J. Geophys. Res.* 105, 19185-19209 (2000).
- Houseman, G., & England, P. Crustal thickening versus lateral expulsion in the Indian-Asian continental collision, *J. Geophys. Res.* 98, 12,233-12,249 (1993).
- Larson, K.M. et al. Kinematics of the India-Eurasia collision zone from GPS measurements. *J. Geophys. Res.* 104, 1077-1093 (1999).
- Lave, J. & Avouac, J.P. Fluvial incision and tectonic uplift across the Himalaya of Nepal. *J. Geophys. Res.* 106, 26561-26591 (2001).
- Le Dain, A. Y., P. Tapponnier, and P. Molnar, Active faulting and tectonics of Burma and surrounding regions, *J. Geophys. Res.*, 89, 453-472, 1984.
- Kidd, W. S. F. & Molnar, P. Quaternary and active faulting observed on the 1985 Academia Sinica-Royal Society geotraverse of Tibet. *Philos. Trans. R. Soc. London, Ser. A* 327, 337–363 (1988).
- King, R. W. & Bock, Y. Documentation for the MIT GPS analysis software: GAMIT, version 9.3, Mass. Inst. of Technol., Cambridge, 1995.
- King, R. W. et al. Geodetic measurement of crustal motion in southwest China, *Geology* 125, 179~182 (1997).
- Molnar, P. & Tapponnier, P. Cenozoic tectonics of Asia: Effects of a continental collision. *Science* 189, 419–426 (1975).
- Molnar, P. & Lyon-Caen, H. Fault plane solutions of earthquakes and active tectonics of the northern and eastern parts of the Tibetan Plateau. *Geophys. J. Int.* 99, 123–153 (1989).
- Murphy, M.A., et al., Southward progaration of the Karakorum fault system, southwest Tibet: Timing and magnitude of slip, *Geology*, 28, 451-454, (2002).
- Paul, J. et al. The motion and active deformation of India. *Geophys. Res. Lett.* 28, 647-650 (2001).
- Reigber, Ch., et al. New space geodetic constraints on the distribution of deformation in Central Asia, *Earth Planet. Sci. Lett.* 191, 157-165 (2001).
- Rowley, D.B. Age of initiation of collision between India and Asia: A review of stratigraphic data. *Earth Planet. Sci. Lett.* 145, 1-13 (1996).
- Royden, L. H. et al. Surface deformation and lower crustal flow in eastern Tibet. *Science* 276, 788~790 (1997).
- Sella, G. F., T. H. Dixon and A. Mao, REVEL: A model for recent plate velocities from space geodesy, *J. Geophys. Res.*, 107, 10.1029/2000JB000033, 2002.
- Shen, Z. K. et al. Contemporary crustal deformation in east Asia constrained by Global Positioning System measurement. *J Geophys Res* 105: 5721~5734 (2000).
- Shen, Z. K. et al. Crustal deformation associated with the Altyn Tagh fault system, western China, from GPS. *J. Geophys. Res.* 106, 30607-30621 (2001).
- Tapponnier, P., Peltzer, G., Le Dain, A. Y., Armijo, R. & Cobbold, P. Propagating extrusion tectonics in Asia: New insight from simple experiments with plasticine. *Geology* 10, 1339–1384 (1982).
- Tapponnier, P. et al. Oblique stepwise rise and growth of the Tibetan Plateau, *Science* 294, 1671-677 (2001).
- Taylor M. et al. Conjugate strike-slip faulting along the Bangong-Nujiang suture zone accommodates coeval east-west extension and north-south shortening in the interior of the Tibetan Plateau, *Tectonics* 22, 1044, doi:10.1029/2002TC001361, (2003).
- Wang, Q. et al. Present-day crustal deformation in China constrained by Global Positioning System (GPS) measurements, *Science* 294, 574-577 (2001).
- Working Group on the Altyn Tagh fault, The Altyn active fault zone, (China Seismological Press, Beijing: 1993).
- Zhang, P. et al., Rate, amount, and style of late Cenozoic deformation of southern Ningxia, northeastern margin of Tibetan Plateau; *Tectonics*, 10, 1111-1129, 1991.
- Zhang, P., et al., Continuous deformation in the Tibetan Plateau from GPS, *Geology*, (accepted), 2004.